frontiers | Frontiers in Marine Science

TYPE Original Research
PUBLISHED 09 January 2023
DOI 10.3389/fmars.2022.1020351

OPEN ACCESS

EDITED BY
Sally Brown,
Environment Agency, United Kingdom

REVIEWED BY
Iris Möller,
Trinity College Dublin, Ireland
Tomasz Labuz,
University of Szczecin, Poland

*CORRESPONDENCE
Björn Mehrtens
b.mehrtens@tu-braunschweig.de

SPECIALTY SECTION
This article was submitted to Coastal Ocean Processes, a section of the journal Frontiers in Marine Science

RECEIVED 16 August 2022
ACCEPTED 09 December 2022
PUBLISHED 09 January 2023

CITATION
Mehrtens B, Lojek O, Kosmalla V, Bölker T and Goseberg N (2023) Foredune growth and storm surge protection potential at the Eiderstedt Peninsula, Germany.
Front. Mar. Sci. 9:1020351.
doi: 10.3389/fmars.2022.1020351

Foredune growth and storm surge protection potential at the Eiderstedt Peninsula, Germany

Björn Mehrtens[1]*, Oliver Lojek[1], Viktoria Kosmalla[1], Thea Bölker[1] and Nils Goseberg[1,2]

[1]Leichtweiß-Institute for Hydraulic Engineering and Water Resources, Division of Hydromechanics, Coastal and Ocean Engineering, Technische Universität Braunschweig, Braunschweig, Germany, [2]Coastal Research Center, Joint Research Facility of Leibniz Universität Hannover and Technische Universität Braunschweig, Hannover, Germany

In the context of climate change and associated sea level rise, coastal dunes can provide an essential contribution to coastal protection against wave attack and flooding. Since dunes are highly dynamic systems, their potential safety levels are related to their long-term development, varying in time and space, however pertinent research that ties those aspects together are generally scarce. The objective of this study is to analyze the long-term development of a young coastal foredune at the Eiderstedt peninsula, Germany and assess its coastal protection potential. This research presents (i) a novel semi-automated *Dune Toe Tracking* (DTT) method to systematically extract dune toes from cross-shore elevation profiles; (ii) established tools to derive the extraction of characteristic dune parameters and (iii) a newly defined *Critical Storm Surge Level* (CSSL) to relate spatio-temporal dune growth with coastal storm surge protection. Based on geospatial survey data, initial dune formation was identified in the 1980s. By 2015, the foredune had developed over a 6.5 km coastal stretch with a mean annual growth of 7.4m^3/m. During the course of dune evolution, the seaward dune toe shifted seaward by an average of 2.3m/yr, while simultaneously increasing in height by an average of 1.1 cm/yr. Overall, the foredune formation established a new line of defense in front of an existing dike/dune line that provides spatially varying protection against a mean CSSL of 3.4m + NHN and can serve as an additional buffer against wave attack during severe storm events.

KEYWORDS

coastal dunes, foredune growth, dune toe tracking, coastal protection, sea level rise, storm surges, fema-rule

1 Introduction

Vegetated coastal dunes are characteristic morphological landforms prevalent along sandy, low-sloped coastlines around the world (Goldstein et al., 2017). Naturally formed on top of the backshore as shore-parallel aligned dune ridges (Hesp, 2002; Durán and Moore, 2013), they contribute various ecosystem services such as biodiversity (Nehren et al., 2016), freshwater provision (Barbier et al., 2011) and recreation (Heslenfeld et al., 2008). In addition, coastal dunes are of vital importance for coastal protection. Low lying dunes provide a first buffer against storm surges and reduce the height of near-shore wave attack (Temmerman et al., 2013). This is caused by increased wave breaking as a result of eroded sand that nourishes the foreshore bathymetry during storm action. In contrast, higher elevated dunes form a barrier to potentially shield the adjacent hinterland from elevated water level and flooding (Keijsers et al., 2015; Maximiliano-Cordova et al., 2021; Van IJzendoorn et al., 2021; Figlus, 2022; Miocic et al., 2022). Furthermore, coastal dunes show a natural capacity for self-repair and post-storm recovery under favorable conditions (Gracia et al., 2018). Several countries apply dune management strategies through sand fences to stimulate dune growth caused by aeolian sand transport (Eichmanns et al., 2021). Therefore, coastal dunes offer multiple adaptive and sustainable benefits compared to traditional hard engineering structures like sea dikes, which require regular maintenance. However, the dynamic development of coastal dunes regarding their geometry and volume (Goldstein et al., 2017) has been shown to result in varying protection levels in time (De Vries et al., 2012) and space (Zarnetske et al., 2015). Meanwhile, climate change and its associated drivers (Wong et al., 2014) such as sea level rise (SLR) (Vousdoukas et al., 2017), intensifying storm surges (Arns et al., 2015) and wave climates (Grabemann et al., 2015; Bell et al., 2017) increase the pressure on coasts (Hallin et al., 2019). These influences are expected to have a major impact on the development of coastal dunes (Van IJzendoorn et al., 2021) and their coastal protection function in the future (Zarnetske et al., 2015).

Coastal dunes develop as a result of erosion and accretion of sand, with the residual aeolian-hydrodynamic transport determining whether dunes are eroding or growing long-term (De Vries et al., 2012; Strypsteen et al., 2019; Gao et al., 2020). Their formation and evolution are driven by complex biophysical feedbacks between vegetation and sediment transport (Hesp, 2002; Durán and Moore, 2013; Zarnetske et al., 2015; Goldstein and Moore, 2016). Incipient foredunes arise due to a continuous supply of aeolian sand-transport, which is trapped and deposited in the vicinity of dune-building vegetation (Durán and Moore, 2013; Goldstein and Moore, 2016) or stimulated by large woody debris (Grilliot et al., 2019; Falkenrich et al., 2021). These foredunes, also called embryonic dunes, can grow up to two meters in height (Montreuil et al., 2013) and characterize the first stage in dune succession (Hesp, 2002; Van Puijenbroek et al., 2017). Depending on the cross-shore width of the beach (Corbau et al., 2015), wind and wave characteristics (Hesp, 1988; He et al., 2022), sediment supply (Davidson-Arnott and Law, 1996; Bauer et al., 2009; Delgado-Fernandez and Davidson-Arnott, 2011) as well as prevailing vegetation (Arens, 1996; Miot da Silva et al., 2008), incipient foredunes can grow further in volume and height, developing into established foredune systems reaching up to 35 m in height (Hesp, 2002; Castelle et al., 2017; Brodie et al., 2019). However, several studies demonstrated that storm events during the formation process can cause major dune erosion and interrupt the growth, with a phase from years to decades to recover pre-storm states (e.g. Houser et al., 2015; Goldstein and Moore, 2016; Castelle et al., 2017). In contrast, Harley et al. (2022) recently revealed that for embayed (protected) coastal sections, extreme storms can result in massive sediment accretion, in turn resulting in an offset of SLR related erosion. Accordingly, the type of coastal system appears to have an impact on the overall feedback between extreme storms and coastal accretion and erosion.

Over the past decades, a wide range of research has been carried out to investigate the impact of extreme storms on beach-dune systems worldwide, focusing on both erosion behavior (e.g. Gencarelli et al., 2008; Maximiliano-Cordova et al., 2021) and ensuing post-storm recovery (e.g. Brantley et al., 2014). Correspondingly, the response of beach-dune systems to storms is usually not spatially uniform, forming alongshore variability during erosion (Tylkowski, 2017; Héquette et al., 2019) and recovery (Castelle et al., 2017).

Complimentary research has been conducted on the development of coastal dunes, spanning different spatial and temporal scales (Brodie et al., 2019). Brodie et al. (2019) mentioned that only few studies examined coastal dune growth on small spatial scales ranging from sub-meters to tens of meters (McLean and Shen, 2006), where local features such as vegetation or buried driftwood might trap wind-blown sand and influence dune growth (Grilliot et al., 2019). Short-time measurements on a scale of hours to months primarily consider the contribution of aeolian sediment transport to dune growth (Dingler et al., 1992; Nordstrom et al., 1996; Arens, 1997; Jackson et al., 2006; Delgado-Fernandez and Davidson-Arnott, 2011; Splinter et al., 2018). However, Strypsteen et al. (2019) suggested that on a decadal timescale short-term fluctuations due to erosion and accretion might average out, potentially rendering annual differences of negligible relevance. So far, numerous studies examined the long-term development of coastal dunes at various locations around the world (e.g. Seeliger et al., 2000; Pye and Blott, 2008; Miot da Silva and Hesp, 2010; Ollerhead et al., 2013; Cohn et al., 2018; Rader et al., 2018). Extensive studies on the development of existing coastal dune stretches covering several kilometers have been conducted by De Vries et al. (2012) on the Dutch

coast and Strypsteen et al. (2019) on the Belgian coast, both revealing linear increases of dune volume in time at a constant rate. Hesp (2013) carried out a study on the development of several separate incipient foredunes over a period of more than three decades. Furthermore, Levin et al. (2017) investigated the formation and establishment of a foredune system over 70 years and related dune activity to local wind and wave conditions.

In order to examine the long-term development of a coastal dune, it is crucial to reliably identify the dune extent, establishing a clear, applicable and accepted definition of its spatial features. Here, the location of the dune toe, also called dune foot, is a key parameter to define the dune profile and derive its morphological development in time and space (Van IJzendoorn et al., 2021). A fact that has been neglected in the past, as the dune toe was commonly defined by a fixed threshold vertical elevation, e.g. at: the Dutch coast at 3 m above the Dutch reference level NAP (De Vries et al., 2012; Donker et al., 2018); the north coast of SW England at 5 m (Masselink et al., 2022); the southwest coast of France at 6 m NGF (official levelling network in mainland France) (Nicolae Lerma et al., 2022); the East Frisian islands in Germany at 3 m above the German reference level NHN (standard elevation zero) (Eichmanns et al., 2021) and the German North Sea at St. Peter-Ording at 2 m + NHN (Hofstede, 1997). Since this definition does not take into account the individual profile of a dune, it is difficult to draw conclusions about long-term dune shifting and ultimately about coastal protection potential. Alternatively, other approaches define the dune toe based on the seaward limit of dune vegetation (Miot da Silva and Hesp, 2010; Hesp, 2013) or on the maximum slope change landward of the shoreline (Splinter et al., 2018; Pellón et al., 2020).

Some authors have already developed different automated analysis approaches to systematically extract characteristic beach and dune parameters from various coastal profiles to facilitate a more objective analysis (e.g. Wernette et al., 2016; Diamantidou et al., 2020). These consistent methods provide a more generic derivation of the dune toe that can be deployed to monitor spatial and temporal dune shifting. Recently, Van IJzendoorn et al. (2021) applied this technique to track cross-shore dune toe positions along the Dutch coast and compared their decadal development to local SLR. They demonstrated a seaward movement of the dune toe of 1 m/yr as well as a linear vertical dune toe translation in the order of 13mm/yr–15mm/yr. While the horizontal shifting indicated an overall accretive dune growth, it was found that the rate of vertical elevation significantly exceeded examined SLR. To capture this correlation, they defined the *Dune Translation Index* (DTI) by dividing the rate of dune toe change by mean SLR. These findings might influence both the impact of projected climate change on coastal dunes and their coastal protection function.

However, none of the referenced works have yet established a practical way to compute a correlation between dune growth and associated storm surge protection potential due to a lack of (i) feature-based, repeatable and established dune analysis procedures; (ii) evaluation of long-term data covering a newly arisen coastal foredune and (iii) widespread, established tools to reliably predict and quantify a protective capacity of coastal dunes. Existing methods for assessing coastal flood risk and protection of coastal dunes rely on various modelling approaches, varying in their complexity as well as their applicability.

Various dune erosion models have been developed and applied in the past, ranging from analytical and empirical models (Bruun, 1962; Kriebel and Dean, 1993; Larson et al., 2004; Van Rijn, 2009; Mull and Ruggiero, 2014) to complex process-based numerical models (Kobayashi et al., 2007; Roelvink et al., 2009) in order to quantify dune retreat and overtopping during storms. Although established numerical models such as XBeach are useful and widely applied tools for simulating beach and dune erosion (e.g. Santos et al., 2019; Dissanayake et al., 2021; Elsayed et al., 2022), Janssen and Miller (2022) pointed out some limitations regarding their widespread implementation in real-time forecasting, concerning the high effort in model initialization, calibration and computational run times. In contrast, existing analytical models typically require significant simplifications in the description of physical processes and certain boundary conditions (e.g. neglecting specific wave characteristics or storm duration effects) (Janssen and Miller, 2022).

However, since their simplicity and limited data requirements make them easy to apply, analytical models are useful engineering tools when long-term, approximate estimations over large areas are required (Larson et al., 2004). Sallenger (2000) defined a widespread conceptual model with four scale regimes to categorize different storm impacts on barrier islands. Although this *Storm Impact Scale* is a useful tool to classify and potentially forecast different processes and magnitudes of impact, it does not consider specific dune volumes and expected volume losses due to erosion (Janssen and Miller, 2022). The significance of dune volume in assessing the vulnerability of coastal dunes was recently pointed out by Itzkin et al. (2021), demonstrating the decisive influence of dune width on erosion behavior during long storm events. Other guidelines such as the FEMA 540-rule consider specific dune volume and can be applied for dune construction and the assessment of dune retreat or removal under storm events (FEMA, 2011). This first-order size criteria evaluates the amount of sand stored within a specific dune section in relation to a 100-year stillwater elevation and neglects other influencing factors such as storm surge duration and wave energy at the seaward dune face. Therefore, this approach is not directed to consider storm events with varying return periods, quantify dune erosion and derive probabilities of failure (Janssen and Miller, 2022).

In order to provide a first analytical approach to relate long-term coastal dune development to coastal protection, this study

investigates a spatio-temporal dune evolution based on field data covering a recently arisen foredune system at the North Sea coast of Schleswig-Holstein, Germany. The investigation has three specific objectives: (1) to develop a semi-automated procedure for objective analysis of key dune parameters based on digital elevation data; (2) to assess the foredune development in the study area and derive specific dune characteristics and (3) to correlate dune formation results with coastal protection potential based on appropriate standards.

2 Materials and methods

2.1 Study area

The coastal foredune system investigated in this study is located along the west coast of the Eiderstedt peninsula, Germany (see Figure 1). This region is situated in the mid-latitudes in Northern Europe, where the North Sea forms a continental shelf sea with the German Bight in the south-eastern area, harboring a diurnal meso-tidal regime with an average tidal range of approximately 3.0 m near the coast (Jänicke et al., 2021). As reported by MELUR (2013), local sea level in the region has risen by an average of 0.18 cm/yr from 1940 to 2007.

The foredune is oriented along a north-south axis and extends over 6.5 km, mostly parallel to the North Sea coast. Seaward in front of the dune stretches a wide sandy beach (with a beach width up to 1.5 km) covering a total area of approximately 7 km^2 (Hofstede, 1997). A sea dike with a mean crest height of 8.0 m + NHN runs landward of the foredune to protect the adjacent hinterland from flooding (MELUR, 2013). However, the dike line is separated along a 1.3 km stretch by an older, established dune system. Furthermore, a natural system of salt marshes and tideways extends in the mid and southern areas between the foredune and the dike/dune line (see Figure 1C).

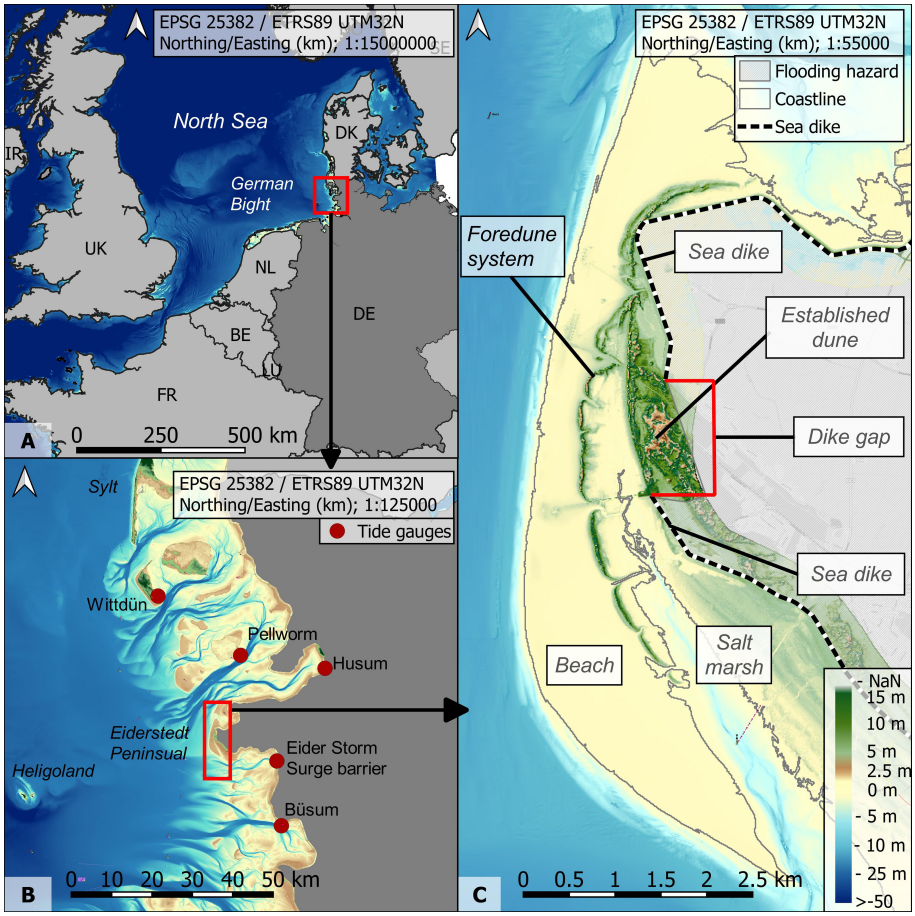

FIGURE 1
Overview map of the study area, with **(A)** location at the North Sea coast; **(B)** location of the Eiderstedt peninsula; **(C)** focus area map with areal characteristics (beach, foredune, salt marsh, dike/dune line). EPSG used is 25382 for all panels; Elevation data obtained through EMODnet Bathymetry Consortium (2020) and Sievers et al. (2020).

This site and its coastal foredune were first addressed by Hofstede (1997), who identified the initial formation of a narrow dune line in the early 1980s. By 1994, the foredune had developed over a length of 4 km at a growth rate of 36 km^3/yr reaching a maximum crest height of 8.7 m + NHN. Simultaneously, the study highlighted the dynamic morphological development of the sandy beach over the period from 1949 to 1994. This process followed several successive erosion and sedimentation phases, with the dry beach area above mean high water growing wider overall and increasing vertically by an average of 0.3 m. According to Hofstede (1997), the expansion of the dry beach was most likely caused by increased sediment supply from the coastal foreshore, potentially exposing a larger area to aeolian sediment transport over the years and promoting the initial foredune growth.

2.2 Data

Geospatial survey data required for the coastal foredune analysis were provided by the Agency for Coastal Protection, National Parks, and Ocean Protection Schleswig-Holstein (LKN.SH) for a total of 13 years from 1949 to 2015, covering more than six decades of coastal development. Except for the first survey in 1949, all data collections have been conducted at similar times over the years (see Table 1). Each geodata survey was consistently performed along several parallel aligned transects (at a constant spacing of 50 m) with oblique orientation to the shoreline over a varying coverage. Until 1988, geospatial data collections were based on terrestrial surveys with similar average resolutions (see Table 1) and vertical inaccuracies of approximately ± 3.0 cm (Hofstede, 1997). In subsequent years, terrestrial survey methods were replaced by Lidar measurements, providing significantly increased resolutions (see Table 1). To analyze local SLR, long-term water level records at several nearby coastal stations were provided by the German Federal Institute of Hydrology (BfG). A total of 5 gauging stations were considered, with the majority covering the entire study period from 1949 to 2015 (see Table 2). In addition, further pre-processed geospatial raster data were obtained from the Federal Waterways Engineering and Research Institute (BAW) EasyGSH-DB portal for the year 2016 with a resolution of 10 m x 10 m (Sievers et al., 2020).

2.3 Methodology

The workflow of our methods is structured in several steps, starting with the analysis of local SLR. Secondly, the preparation and processing of geospatial data is outlined. Based on this, the following sections provide a detailed description concerning the analysis of the shoreline and the foredune. As a final step in the workflow, the storm surge protection analysis of the foredune is outlined.

2.3.1 SLR analysis

In order to assess local SLR at the Eiderstedt peninsula (cp. Figure 1B), the provided water level records (see Table 2) were analyzed over the period from 1949 to 2015, extracting temporal

TABLE 1 Overview of available geospatial data covering the study area.

No.	Date	Coverage	Mean resolution	Median resolution	Source	Data type
1	15-01-1949	8.6 km^2	39.0 m	23.9 m	LKN.SH	Terrestrial survey
2	15-07-1958	9.1 km^2	38.5 m	23.4 m	LKN.SH	Terrestrial survey
3	15-07-1964	11.3 km^2	38.5 m	22.6 m	LKN.SH	Terrestrial survey
4	15-07-1971	12.1 km^2	39.1 m	24.1 m	LKN.SH	Terrestrial survey
5	15-07-1980	12.3 km^2	38.9 m	23.7 m	LKN.SH	Terrestrial survey
6	15-07-1981	12.2 km^2	38.9 m	23.6 m	LKN.SH	Terrestrial survey
7	15-07-1984	11.3 km^2	38.7 m	23.3 m	LKN.SH	Terrestrial survey
8	30-06-1985	11.9 km^2	38.9 m	23.7 m	LKN.SH	Terrestrial survey
9	15-07-1987	14.2 km^2	38.1 m	22.5 m	LKN.SH	Terrestrial survey
10	15-07-1988	13.7 km^2	38.7 m	23.0 m	LKN.SH	Terrestrial survey
11	15-05-2005	12.0 km^2	5.0 m	2.4 m	LKN.SH	Lidar survey
12	20-05-2010	11.1 km^2	5.3 m	2.0 m	LKN.SH	Lidar survey
13	13-07-2015	11.4 km^2	8.4 m	2.6 m	LKN.SH	Lidar survey
14	2016	21.6 km^2	10.0 m	10.0 m	BAW	Synoptic raster data

TABLE 2 Overview of water level records measured at 5 nearby coastal stations.

No.	Coastal station	Year	Source	Data type
1	Wittdün	1935 to 2021	BfG	High tides; Low tides
2	Pellworm	1977 to 2021	BfG	High tides; Low tides
3	Husum	1935 to 2021	BfG	High tides; Low tides
4	Eider storm surge barrier	1972 to 2021	BfG	High tides; Low tides
5	Büsum	1935 to 2021	BfG	High tides; Low tides

trends at an annual resolution. First, average annual water levels were determined for each coastal station by averaging the respective high and low tide values. Thereby, only those years were considered in which at least 95% of the tidal data was reliably recorded. Subsequently, mean annual water levels were calculated using 5 coastal stations and applied to perform a linear regression. In addition, the high tide values were also used for a trend analysis of mean high water (MHW).

2.3.2 Geodata processing

Digital elevation models (DEMs) form the basis of our analysis. The geospatial survey data sets from 1949 to 2015 were provided as xyz-point data format and processed using Quantum Geo Information System (QGIS), Version 3.10 and Mathworks Matrix Laboratory (MatLab), Version R2020a. Initially, the data was screened regarding the coverage of our study area, including the sandy beach, the foredune as well as the landward dike/dune line. Only if data coverage was sufficient and all three areas were at least partially covered by an individual data set for a given year, the data was considered and evaluated. Subsequently, a regular grid was generated, spanning the focus area 2.55 km east-west and 6.66 km north-south, with a regular grid raster cell size of 1.0 m (similar to Donker et al., 2018; Nicolae Lerma et al., 2022), resulting in 169 830 cells per DEM. Elevation data was then interpolated onto the regular grid cells using a Delaunay triangulation. Excess data outside the defined regular gridded area was discarded for further processing.

A total of 13 annual surveys were processed to yield homogeneous DEMs for subsequent analyses. Resulting DEMs were checked for vertical deviation by means of inverse-triangulation, querying the interpolated surface elevation of an individual DEM for a given year at the available surveyed coordinates provided by the LKN.SH for that year. Elevation values have been compared on a point-by-point basis. A cumulative distribution function was evaluated for both, the raw survey data and corresponding triangulated DEM. Finally, the least squares method has been applied to calculate the absolute elevation error per data set.

Within the gridded area, a 6.4 km long geotransect was defined using QGIS, following the curvature of the foredune crests along its north-south axis. From this transect, orthogonal evaluation profiles were constructed numerically with a profile length of 1.4 km, crossing the foredune and the beach before ending around the 3.0m iso-depth contours (see Figure 2B). All evaluation profiles were constructed 1.0m apart, resulting in a total of 6394 profiles, with consecutive numbering starting in the south. Finally, the horizontal elevation distances of the individual profiles were consistently interpolated to 1.0m.

2.3.3 Shoreline analysis

The processed elevation profiles were used to analyze the shoreline in order to relate its development to the analysis of the foredune growth. In this study, the shoreline location was defined as the furthest landward intersection seaward of the dune crest between an elevation profile and mean high water. For this purpose, the previously analyzed mean high water trend from 1949 to 2015 provided year-specific high water levels taking sea level rise into account. The cross-shore position of the shoreline was analyzed for each elevation profile using year-specific mean water level over the study period from 1949 to 2015.

2.3.4 Dune analysis

In order to reliably extract the foredune location along an elevation profile, it is primarily important to identify the dune extent. As mentioned in the introduction, dune toe positions in the study area have previously been defined at a fixed vertical elevation at 2.0m above NHN (Hofstede, 1997), although this limits the ability to track their long-term horizontal and vertical movement. Therefore, a novel semi-automated dune toe tracking (DTT) method was developed to detect seaward and landward dune toes based on specially defined criteria.

The detection procedure consists of several steps and specific criteria (see Figure 3) that were tested and defined within the framework of this study. In the first step, the dune crest was defined as the maximum peak along an elevation profile. To avoid uncertainties and deviations in the detection of shallow peaks, we thereby specified a minimum threshold of 0.5m above mean high water. Although the initial formation of small embryo dunes (< 2m) can thus not be exactly identified, this fact was negligible in the context of this study and the subsequent derivation of coastal protection potential. If no dune crest was found along a profile, the detection procedure stopped after the first step and returned a “no-dune”-statement for the corresponding profile.

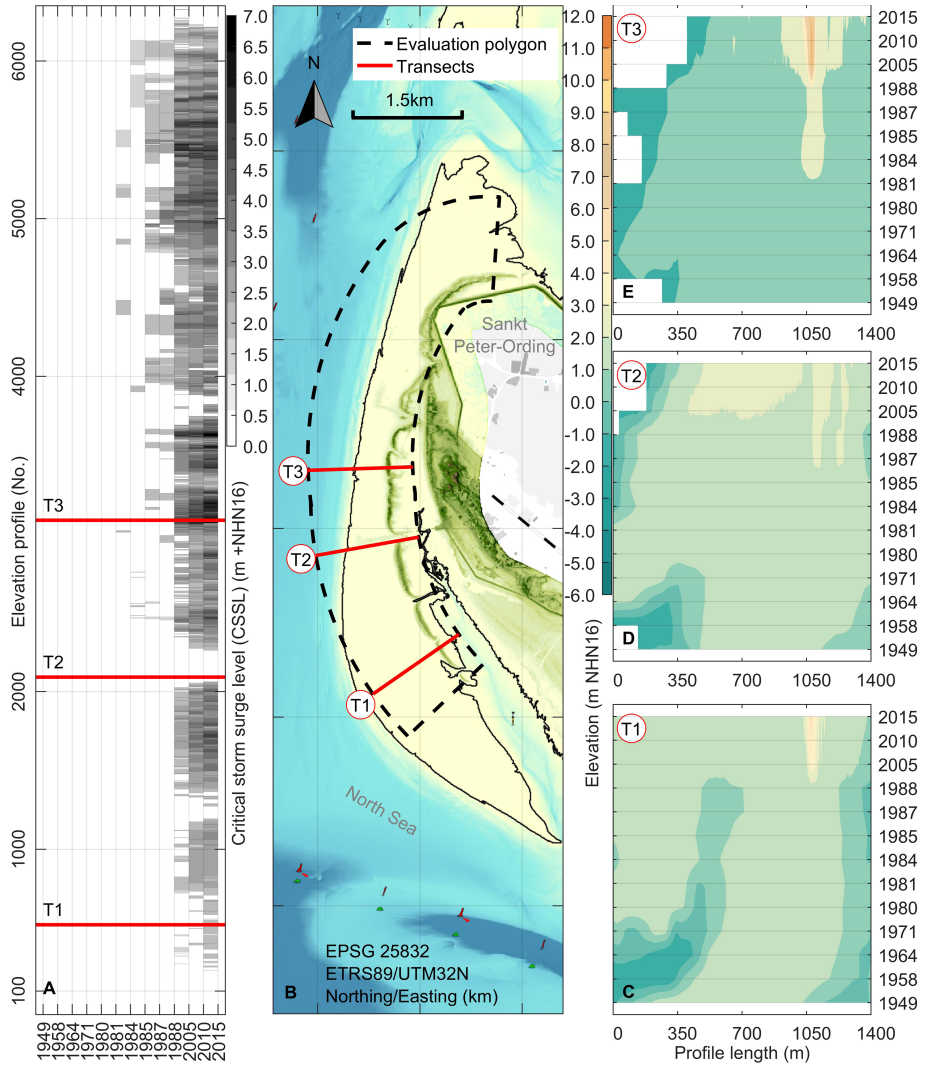

FIGURE 2
Overview of geospatial processing and the foredune analysis with **(A)** Analyzed FEMA-540 rule related critical storm surge level protection; **(B)** overview map with constructed normal elevation profiles along the foredune; **(C–E)** Hovmoeller-diagrams of 3 selected profiles. Geolocations are highlighted in **(B)**.

Secondly, we developed an iterative search algorithm to consistently find the position of the seaward dune toe along a profile. Starting from the dune crest, the first position seaward of the crest that fulfills the following criteria (a–c) was defined as the seaward dune toe: (a) the elevation at the position must exceed the calculated mean high water in order to neglect potential offshore sandbars below the dry beach level; (b) the deviation from mean elevation over a specific cross-shore distance Δx must not exceed 0.1% of the corresponding distance; (c) the sum of all identified elevation deviations over the specific cross-shore distance Δx must not exceed 0.1% of the corresponding distance. To select the best fitting specific distance Δx for our study area, we performed several test runs with distance values of 25m, 50m, 75m, 100m, 150m and 200m. After each test run, we calculated the respective number of elevation profiles in which no dune toe was detected. Afterwards, the detected dune toes were further examined to identify potential outliers where dune toes were detected at deviating locations (e.g. due to multiple dune ridges along a profile). Similar to the first step, we defined a dune absence if no toe was properly detected and terminated the procedure for the corresponding profile.

Thirdly, the landward dune toe was defined as the first location landward of the dune crest that intersects the previously

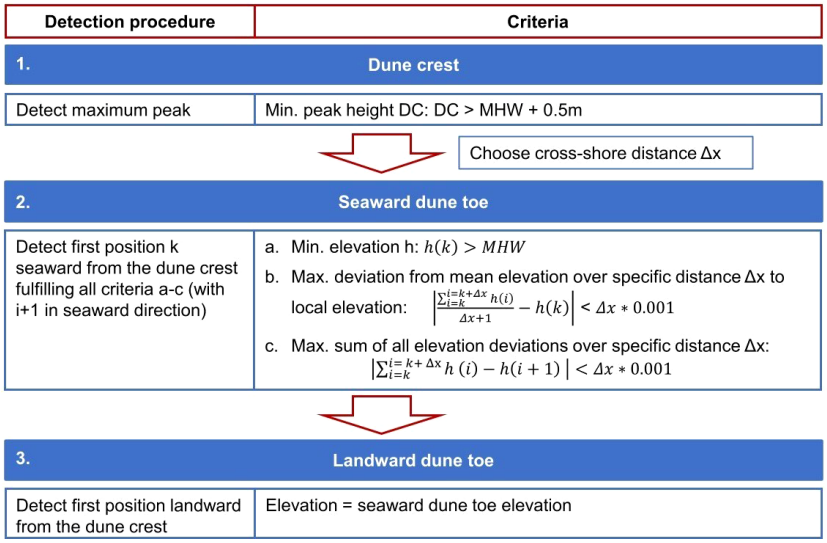

FIGURE 3
Structure diagram of the semi-automated DTT method.

detected seaward dune toe elevation. This simplified assumption was made since the detection algorithm from step two was not suitable for finding accurate landward dune toes due to the bordering salt marsh as well as the dike/dune line (cp. Figure 1C). If no landward dune toe was detected due to an elevated landward profile above the height of the seaward dune toe, this parameter was neglected.

Building on the dune toe detection applied for each elevation profile, characteristic trigonometric dune parameters were determined to identify the spatio-temporal development of the foredune. As shown in Figure 4A, the dune height equals the vertical difference between the dune crest and the seaward dune toe. The dune volume per elevation profile results from a numerical integration of the cross-section area above the corresponding toes. If no landward dune toe existed, the dune volume was not determined. Furthermore, a simplified seaward dune slope (also called upwind slope) was determined according to the respective spatial gradient between the seaward dune toe and the dune crest. Finally, evolution trends were derived for various parameters. First, each elevation profile was considered individually by calculating the trend of each individual parameter between the earliest and latest detected values in time. Subsequently, a median value, a mean value as well as the mean 95% confidence interval was calculated for the corresponding parameter from all available profiles.

2.3.5 Storm surge protection analysis

We applied an analysis for the coastal protection potential that was based on the FEMA-540 rule, the established size criterion for coastal dunes provided by the Federal Emergency Management Agency (FEMA, 2011). This criterion defines the amount of sand stored within the cross-sectional area of the frontal half of a dune above the 100-year stillwater elevation (SWEL) as the critical parameter for protection against a 100-year storm event. As long as this critical area contains at least 540 cubic feet of sand per linear foot (approximately 50m^3/m), the coastal dune is expected to withstand a 100-year storm. Otherwise, if the required amount of sand in the cross-sectional area is insufficient, the dune erodes and forms a low, gently sloped profile that subsequently fails to provide significant coastal protection (Wootton et al., 2016).

In this study, the FEMA-540 rule was applied for the first time, to our knowledge, to scientifically examine how the protection potential of a coastal dune evolves depending on its spatio-temporal growth. The FEMA approach was chosen as, in contrast to the other analytical and numerical models mentioned earlier, it allowed a relatively quick and straightforward protection assessment by considering only the cross-sectional profile of a dune and neglecting other influencing factors such as wind and wave characteristics. This enabled the respective protection potential to be determined along the previously defined elevation profiles for all years considered in this study.

Using the previously analyzed dune characteristics, the first step of the FEMA-540 procedure is to set a vertical line starting from the identified dune crest. This line marks the fixed vertical limit of the frontal half of the dune (see Figure 4B). In the next step, the standard FEMA-540 rule was partially modified and extended to not exclusively consider 100-year storm events. Instead, the criterion was applied to calculate the corresponding frontal dune area above different storm surge

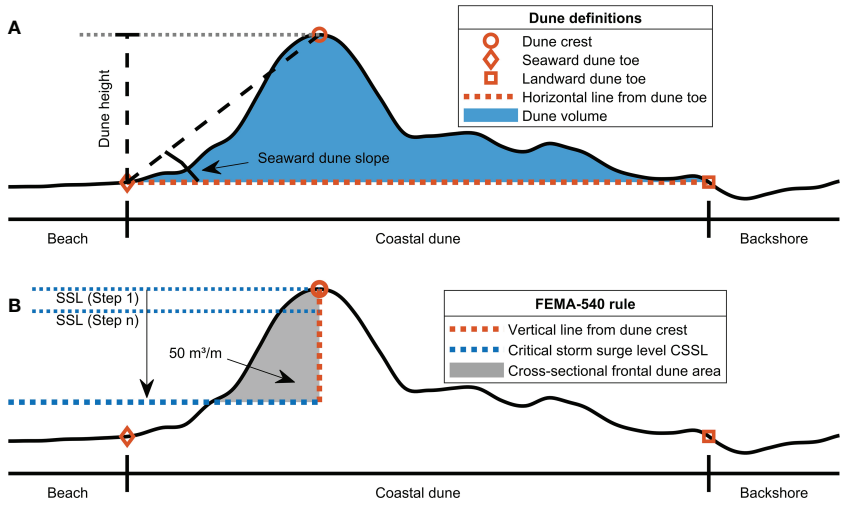

FIGURE 4
Definition of **(A)** specific dune parameters and **(B)** the determination of the CSSL using the adapted FEMA 540-rule.

levels (SSLs). This was done to iteratively deduce at which water level the minimum required threshold of 50m^3/m is fulfilled or undercut. The first SSL during the iteration always equals the detected height of the dune crest. Subsequently, the SSL is reduced with an increment of 0.01m and the corresponding frontal dune area is determined. This iterative process continues until the minimum required threshold of 50m^3/m is reached for a certain SSL or the water level equals the seaward dune toe elevation and the iteration is automatically stopped. If the threshold of 50m^3/m is reached, the corresponding SSL is subsequently defined as the critical storm surge level (CSSL) (see Figure 4B). Accordingly, the CSSL defines the maximum SSL up to which a sufficient amount of sand is stored within the frontal half area to provide a verified storm surge protection. In contrast, for SSLs exceeding the CSSL, the corresponding amount of sand in the area would not assure adequate protection. If no CSSL is determined throughout the iteration, the dune contains insufficient sand volume between the seaward dune toe and the vertical line at the dune crest to offer protection against minimum water level (defined here as no protection).

3 Results

3.1 Local sea level rise

Figure 5 shows the trend analyses of mean sea level and mean high water along the coast of the Eiderstedt peninsula determined from 5 different coastal stations (cp. Figure 1B) from 1949 to 2015. Although average annual water levels show considerable fluctuation throughout the years, both linear regressions reveal significant trends. Over the period from 1949 to 2015, local sea level has risen linearly at an overall rate of 0.25 cm/yr, while mean high water shows an increased positive trend of 0.38 cm/yr. These trends are consistent with findings by Jänicke et al. (2021), who demonstrated tidal range increases of approximately −0.05 cm/yr to 0.5 cm/yr in the study area (coastal stations: Wittdün, Husum, Büsum) from 1958 to 2014. Furthermore, Jensen (2020) reported a lower mean sea level increase of 0.15 cm/yr at the coastal stations Husum and Büsum from 1934 to 1983, indicating potentially accelerated SLR in recent decades.

3.2 Foreshore evolution

Figures 6A–D present the spatio-temporal evolution of the shoreline. Over the period from 1949 to 2015, the shoreline experienced a highly dynamic development, characterized by various phases of retreat and progradation. Despite a slight tendency of retreat in earlier years, the shoreline tended to prograde seaward by an average of 2.3m/yr from 1949 to 1981. This coincides with findings by Hofstede (1997), who observed a distinct beach width growth during this period, potentially caused by periodic sandbar migration promoting an increased sediment supply to the foreshore. In the following decades until 2015, this development reversed and the shoreline retreated landward, resulting in an overall mean shoreline retreat of 1.5m/yr from 1949 to 2015. Apart from potential changes in sandbar migration, local SLR is a potential driver for increased shoreline erosion (Mariotti and Hein, 2022).

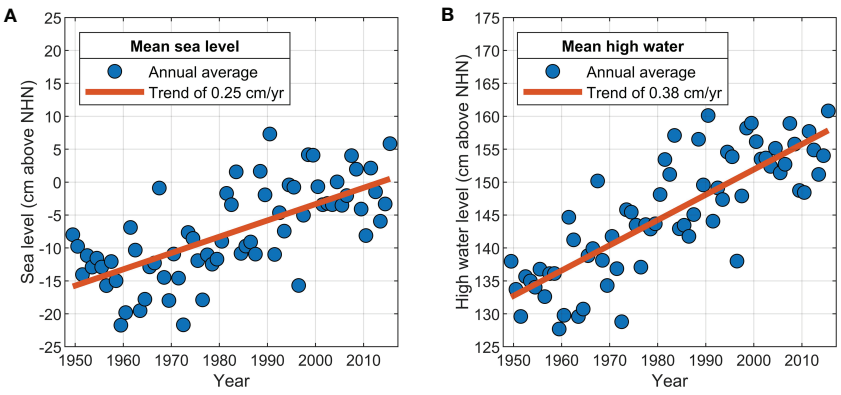

FIGURE 5
Trend analysis of annual average values of five coastal stations (Wittdün, Pellworm, Husum, Eider storm surge barrier, Büsum) for **(A)** mean sea level and **(B)** mean high water.

3.3 Seaward dune toe detection

The semi-automated DTT method has been executed several times using different cross-shore distances Δx to evaluate which distance is most applicable for the study area. Figures 7A, B contain all detected seaward dune toe positions and elevation heights in 2015 for the tested distances Δx of 25m, 50m, 75m, 100m, 150m and 200m. For all distances examined, the detection algorithm identified dune toes in a majority of the 6394 elevation profiles (see Figure 7E). Thereby, the longest cross-shore distance Δx of 200m resulted in the highest number of elevation profiles with undetected dune toes. Furthermore, the spatial comparison in Figures 7A, B as well as the exemplary elevation profile in Figure 7C demonstrate that the dune toes tend to be detected further seaward and accordingly lower for shorter distances Δx.

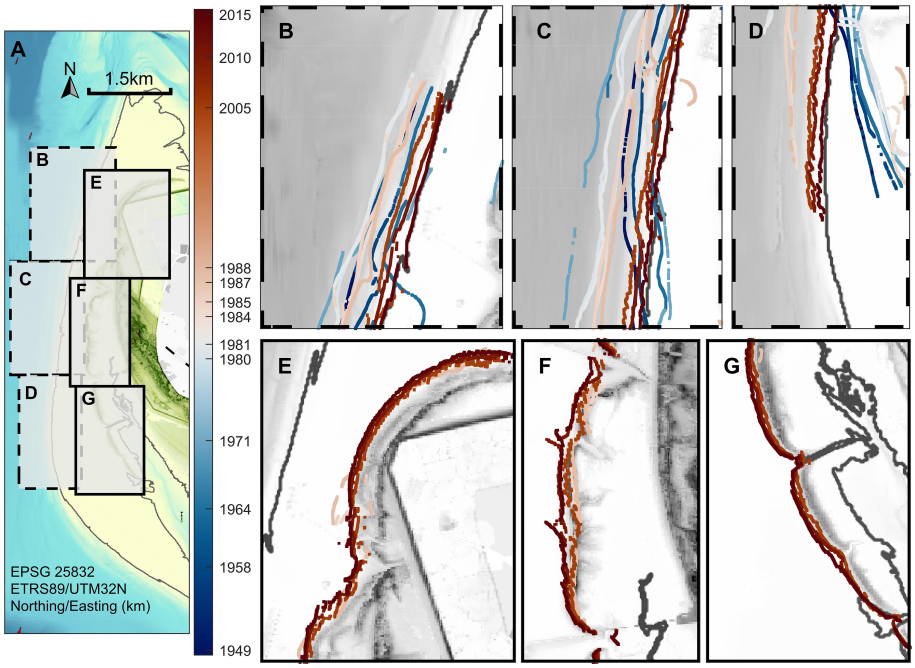

FIGURE 6
Subdivision of the study area **(A)** and spatio-temporal development of **(B–D)** the shoreline location and **(E–G)** the seaward dune toe position.

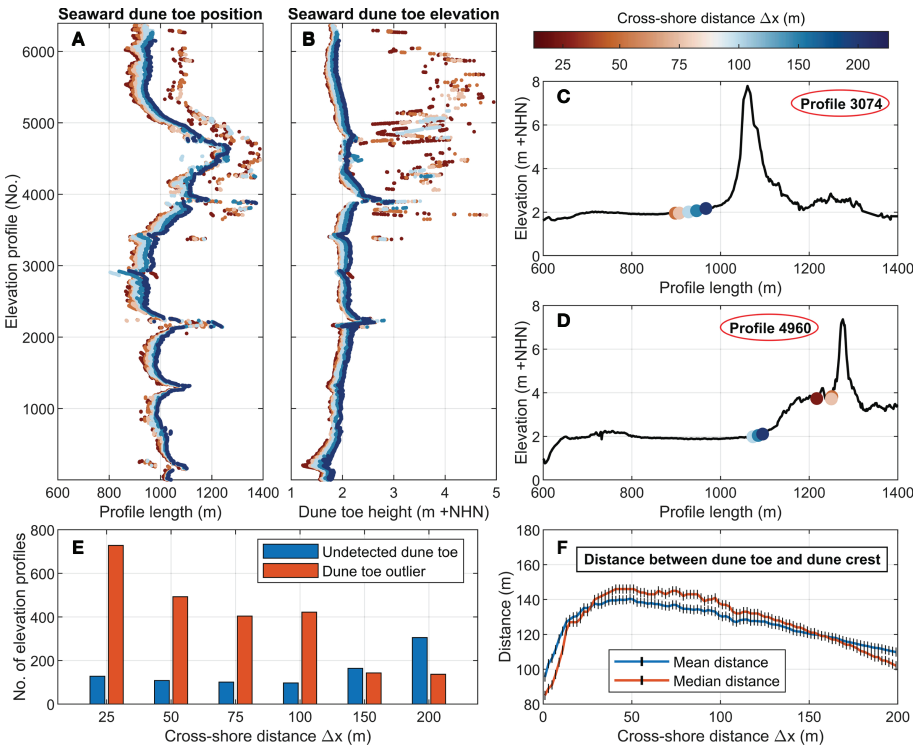

FIGURE 7
Performance evaluation of different specific cross-shore distances Δx in 2015 with **(A)** the positions of all detected seaward dune toes; **(B)** the heights of all detected seaward dune toes; **(C, D)** two exemplary elevation profiles; **(E)** a statistic of undetected and deviant dune toes per Δx; **(F)** mean and median distances between the seaward dune toe and the dune crest per Δx.

Particularly in the central and northern regions of the study area, numerous dune toes were detected further landward at elevation heights above 2.5m + NHN and considerably deviating from identified dune toes in the surrounding profiles. These deviating dune toes (referred as dune toe outliers) increasingly occurred for specific distances of less than 150m (see Figure 7E). As shown in the exemplary profile in Figure 7D, the foredune shape in this region is partially characterized by an elevated seaward dune slope with several small dune ridges. As a consequence, for shorter distances Δx dune toes were already located at these sections, whereas for longer distances dune toes were properly detected in the beach-dune transition area. Overall, the specific cross-shore distance Δx of 150m resulted in the lowest total number of undetected dune toes and outliers (see Figure 7E). In addition, Figure 7F demonstrates that the mean and median distances between the located dune toes and dune crests along all elevation profiles had a comparable high agreement at a distance Δx of 150m. Therefore, a cross-shore distance Δx of 150m was applied for the entire dune toe tracking.

In order to compare the applied DTT method with existing procedures, two additional detection algorithms were applied and analyzed for the study area. Besides the commonly used method with a fixed threshold elevation at 2.0m + NHN (Hofstede, 1997), dune toes were also extracted applying the second derivative method by Diamantidou et al. (2020). Figure 8 compiles all detected dune toe positions and heights in 2015 for the three applied methods, including two exemplary profiles. A comparison of the DTT method with the fixed vertical threshold method shows that the detected dune toe positions were often located relatively close to each other (see Figure 8A). Since the beach system has an approximate height of 2.0m + NHN in wide areas, dune toes were often extracted at similar positions (see exemplary profile in Figure 8C). However, since the method defines all dune toes at a specified threshold height of 2.0m + NHN (see Figure 8B) regardless of the shape of the beach-dune profile, significant deviations occurred in areas with elevated beach profiles as dune toes were detected at large distances from the foredune (see exemplary profile in Figure 8D). In contrast, the dune toes extracted by the second derivative method featured large spatial variations (see Figure 8A) as the detected toes were often located directly at the shoreline or at shallow peaks along the wide beach system (see Figure 8D). As shown in Figure 8C, the algorithm identified a dune toe at the beach-dune transition only when the cross-shore profile contained a relatively smooth beach section.

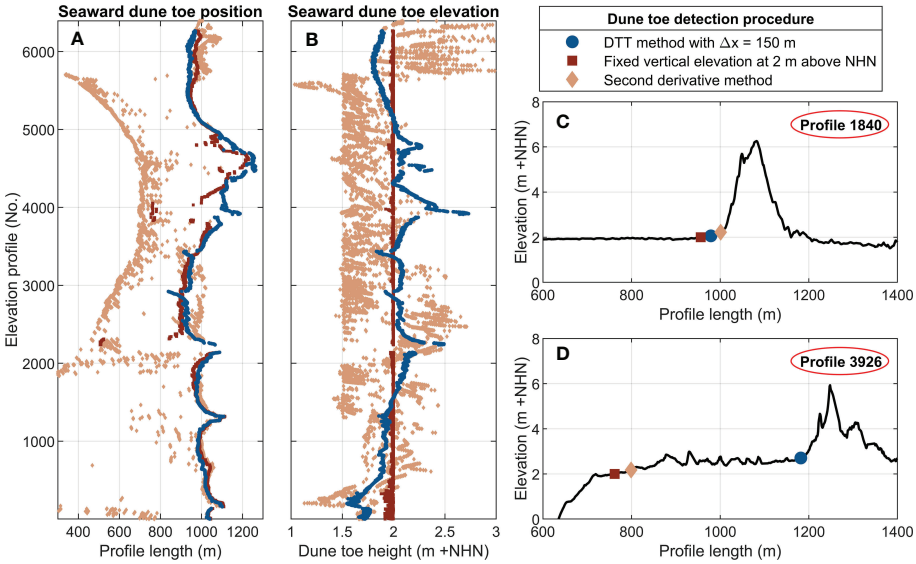

FIGURE 8
Comparison of detected seaward dune toes in 2015 using three different detection procedures with **(A)** the positions of all detected seaward dune toes; **(B)** the heights of all detected seaward dune toes; **(C, D)** two exemplary elevation profiles.

3.4 Foredune development

Building on the detected seaward dune toes (using the DTT method with a cross-shore distance Δx of 150m) and the subsequent analysis of characteristic dune parameters over the years, a first dune formation was identified in 1984, extending over 16% of the considered elevation profiles (see Table 3) and predominantly located along the central and northern sections of the study area (see Figures 6E, F). The initial formation process also becomes apparent when considering the three exemplary profiles T1–T3 shown in the Hovmoeller diagrams (see Figures 2C–E) as well as in Figures 9A–C and Table 4. Whereas the foredune initially developed along the profile T3 in 1984 (see Figures 2E, 9A), Figures 2C, 9C show a delayed foredune formation in the more southern profile T1. This coincides with findings by Hofstede (1997), who observed an incipient foredune formation in front of the established dune system in the early 1980s. Temporally, the dune formation occurred directly after the analyzed period of shoreline progradation and beach growth, potentially increasing the fetch length for aeolian sediment transport and promoting foredune development.

In subsequent years until 1988, the foredune expanded northward and southward along the interface between the beach and the salt marsh covering 47.2% of the analyzed profiles (see Table 3), while reaching a mean dune height of 1.7m and mean dune volume of 81.0m^3/m (see Figure 10). As shown in Figure 10, no storm surge events occurred during this period, potentially causing major dune erosion and interrupting the initial dune growth. The dune growth progressed until the end of the study period in 2015, resulting in a widely developed foredune system covering 95.2% of the examined 6394 elevation

TABLE 3 Percentage of elevation profiles for which dune parameters were identified by the applied detection algorithm for each study year (given in % relative to the total number of 6394 elevation profiles).

Coastal parameter	1949-1981	1984	1985	1987	1988	2005	2010	2015
Dune crest	0.0	16.0	27.3	45.9	47.2	94.5	95.8	95.2
Seaward dune toe	0.0	16.0	27.3	45.9	47.2	94.5	95.8	95.2
Dune height	0.0	16.0	27.3	45.9	47.2	94.5	95.8	95.2
Landward dune toe	0.0	7.7	13.6	21.1	20.2	59.9	60.5	62.9
Dune volume	0.0	7.7	13.6	21.1	20.2	59.9	60.5	62.9
CSSL	0.0	5.4	6.9	23.1	25.2	66.2	77.7	85.5

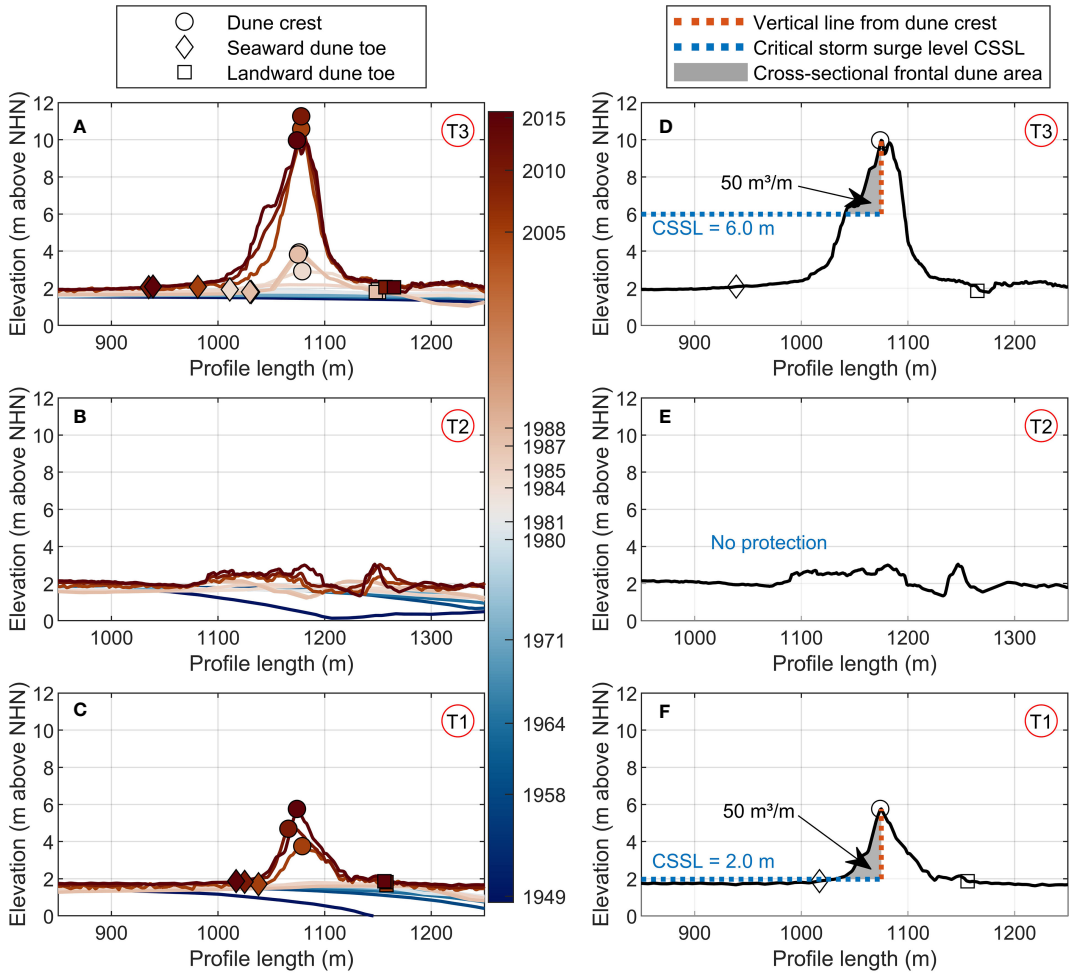

FIGURE 9
(A–C) Foredune development along the selected elevation profiles T1–T3; **(D–F)** identified CSSLs in 2015 at the selected elevation profiles T1–T3.

profiles (see Table 3). In 2015, the foredune reached a mean crest elevation of 6.2m + NHN (or a mean dune height of 4.2m) and gained a mean dune volume of 256.8m^3/m (see Figure 10). As Figure 10 also illustrates, both parameters increased largely linear (with a correlation coefficient R of 0.98), although the percentage of identified values differed from each other (e.g. in 2015 with 95.2% dune crests compared to 62.9% volumes) due to less detected landward dune toes (see Table 3). Over the period from 1984 to 2015, the foredune has grown with a mean dune crest increase of 12.5 cm/yr and a mean volume increase of 7.4m^3/m/yr (see Table 5).

Furthermore, the detected seaward dune toes were investigated with respect to their spatial development. Figures 6E–G demonstrate the seaward dune toe movement over the years. Overall, the dune toes prograded towards the sea by a mean of 2.3m/yr (see Table 5). Simultaneously, the mean dune toe elevation increased over the years from 1.8m + NHN in 1984 (or 1.7m + NHN in 1985) to 2.0m + NHN in 2015 (see Figure 10). This result matches precisely the conventional fixed vertical threshold elevation in St. Peter-Ording at 2.0m + NHN (Hofstede, 1997). On average, the seaward dune toe elevation increased by 1.1 cm/yr over the period from 1984 to 2015 (see Table 5). Since the landward dune toe was determined in a simplified approximation based on the seaward dune toe, its development was neglected during the evaluation.

As illustrated in Table 5, the foredune development featured large spatial variations, ranging from scattered dune recessions to large growth rates above-average. The detected dune crest ranges from 11.2m + NHN in 2010 (see profile T3 in Figures 9A, 2E) to sections with maximum peak heights less than 0.5m above mean high water (see profile T2 in Figures 9B, 2D). Consequently, several gaps (mainly blowouts and passages) split the foredune line over a

10.3389/fmars.2022.1020351

TABLE 4 Analyzed dune parameters for the selected elevation profiles T1–T3 from 1949 to 2015.

	Elevation profile T1							
Coastal parameter	1949-1981	1984	1985	1987	1988	2005	2010	2015
Dune crest (m +NHN)	–	–	–	–	–	3.8	4.7	5.8
Seaward dune toe location (m)	–	–	–	–	–	1038	1025	1017
Seaward dune toe height (m +NHN)	–	–	–	–	–	1.7	1.8	1.9
Dune height (m)	–	–	–	–	–	2.1	2.9	3.9
Landward dune toe location (m)	–	–	–	–	–	1158	1158	1156
Landward dune toe height (m +NHN)	–	–	–	–	–	1.7	1.8	1.9
Dune volume (m^3/m)	–	–	–	–	–	92.8	124.4	148.1
CSSL (m +NHN)	–	–	–	–	–	–	–	2.0
	Elevation profile T2							
Coastal parameter	1949-1981	1984	1985	1987	1988	2005	2010	2015
Dune crest (m +NHN)	–	–	–	–	–	–	–	–
Seaward dune toe location (m)	–	–	–	–	–	–	–	–
Seaward dune toe height (m +NHN)	–	–	–	–	–	–	–	–
Landward dune toe location (m)	–	–	–	–	–	–	–	–
Landward dune toe height (m +NHN)	–	–	–	–	–	–	–	–
Dune volume (m^3/m)	–	–	–	–	–	–	–	–
CSSL (m +NHN)	–	–	–	–	–	–	–	–
	Elevation profile T3							
Coastal parameter	1949-1981	1984	1985	1987	1988	2005	2010	2015
Dune crest (m +NHN)	–	2.9	–	3.9	3.8	10.6	11.2	10.0
Seaward dune toe location (m)	–	1011	–	1031	1030	981	935	939
Seaward dune toe height (m +NHN)	–	1.9	–	1.8	1.8	2.1	2.1	2.1
Dune height (m)	–	1.0	–	2.1	2.0	8.5	9.2	7.9
Landward dune toe location (m)	–	1150	–	1151	1148	1157	1157	1165
Landward dune toe height (m +NHN)	–	1.9	–	1.8	1.8	2.1	2.1	2.1
Dune volume (m^3/m)	–	70.1	–	85.5	86.6	327.8	411.2	447.2
CSSL (m +NHN)	–	–	–	–	–	5.8	6.3	6.0

combined total length of 307m in 2015 (according to 4.8% of the elevation profiles).

The final results of the dune analysis compromise the temporal formation of the seaward dune slope, defined as the gradient between the seaward dune toe and the dune crest. Table 5 demonstrates that the average dune slope steepened during the progressive dune growth. Thereby, the initial average slope of 0.57° increased by a mean of 0.02°/yr. In 2015, the foredune reached a mean seaward dune slope of 2.5° (95% confidence interval between 2.47° and 2.53°), which is within the characteristic range (1°–8°) of a foredune (Sloss et al., 2012).

3.5 Storm surge protection potential

The dune analysis results enabled an assessment of the spatio-temporal coastal protection potential of the foredune by applying the previously outlined FEMA procedure. As shown in Figure 2A, the analysis has been conducted for all elevation profiles over the study period from 1949 to 2015 by determining the respective CSSLs. The results demonstrate an overall increase in CSSL over the years revealing enhanced protection against storm surges along the foredune. In earlier decades, no protective effect particularly against the attack of storm waves

TABLE 5 Overview of analyzed parameter trends over the period from 1984 to 2015, including median values, mean values, the range of each data set and the mean 95% confidence interval.

Period 1984 to 2015				
Coastal parameter	Median	Mean	Range	95% confidence interval
Shoreline retreat (m/yr)	2.8	1.5	−5.7 to 11.2	1.4 to 1.5
Dune crest (cm/yr)	12.9	12.5	−9.0 to 31.5	12.3 to 12.6
Dune height (cm/yr)	11.7	11.3	−12.0 to 31.4	11.2 to 11.5
Dune volume (m^3/m/yr)	8.2	7.4	−22.8 to 24.5	7.3 to 7.6
Seaward dune toe elevation (cm/yr)	1.1	1.3	−2.6 to 11.1	1.1 to 1.2
Seaward dune toe progradation (m/yr)	2.1	2.3	−6.0 to 20.0	2.3 to 2.4
Seaward dune slope (°/yr)	0.03	0.02	−0.50 to 0.25	0.02 to 0.03
CSSL (cm/yr)	7.0	7.8	−15.5 to 38.8	7.6 to 8.0

existed yet, as the initial dune formation appeared in 1984 (see Table 3). In 1985, only 6.9% of the elevation profiles (441 of 6394 profiles) provided an identifiable initial protection against a mean CSSL of 1.5m + NHN (see Figure 10). This is caused by predominantly insufficient dune volume in most elevation profiles at this time. In subsequent years, the spatially limited protection against relatively low CSSLs expanded northward along the foredune, as a direct consequence of dune growth and the associated increase in frontal dune area (see Figure 2A).

Due to further successive dune growth, this progression continued during the subsequent years and decades. In 2015, 85.5% of the 6394 elevation profiles (see Table 3) offered a verifiable protection against a mean CSSL of 3.4m + NHN (see Figure 10). Storm surge protection tends to be highest in the middle and northern part of the study area, mainly caused by the earlier dune evolution seaward of the established dune system (see Figure 2A). Due to the dune formation and volume increase, some profiles provide a potential protection against CSSLs up to 6.0m + NHN (see profile T3 in Table 4, Figure 9D). In contrast, the foredune offers less protection in the south of the study area. Thus, in profile T1, a first protective effect was observed in 2015 against a relatively low CSSL in the range of the seaward dune toe elevation (see Table 4 and Figure 9F).

Overall, the mean CSSL increased largely linearly (see Figure 10) in elevation at a mean rate of 7.8 cm/yr (see Table 5), enhancing storm surge protection over time. Since this trend directly depended on the dune volume growth, both average parameter increases featured a high correlation R of

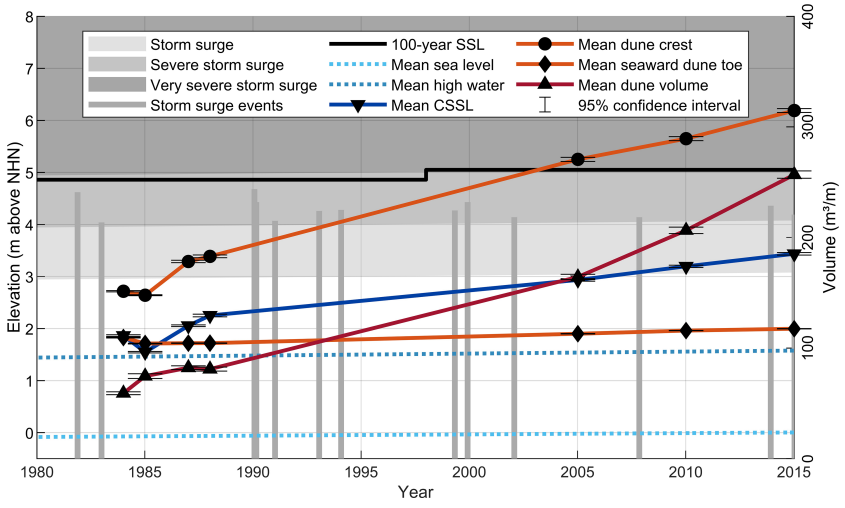

FIGURE 10
Development of average specific dune parameters compared to typical storm surge classes at the German North Sea coast, historical severe storm surge events in the study area and the local 100-year SSL with a defined increase in 1998.

0.95. However, consistent with the previously identified spatial variations in dune height and volume along the foredune, the system does not offer a continuous protection over all 6394 elevation profiles (Figure 9E). In 2015, 14.5% of the analyzed profiles provided no verified protection against a specific CSSL (see Table 3). Figure 2A demonstrates that these discontinuities mainly occur alongside several gaps with widths up to 191m (elevation profile 2114 to 2305).

Finally, Figure 10 illustrates the development of the mean CSSL in comparison to maximum water levels of historical severe storm surge events as well as typical storm surge classes defined at the North Sea coast. According to Jensen and Müller-Navarra (2008), a storm surge ranges from 1.5m to 2.5m above mean high water, a severe storm surge from 2.5m to 3.5m above mean high water and a very severe storm surge over 3.5m above mean high water. Furthermore, the local 100-year SSL of 5.05m + NHN with a minor increase in 1998 (according to MLR, 2001; MELUR, 2013) is also inserted. In 2015 the mean CSSL ranges within the defined storm surge range. As already mentioned, some sections in the study area also provide protection against CSSLs higher than 5.0m + NHN (see exemplary profile T3 in Figure 9D), reaching the 100-year SSL as well as the very severe storm surge class and realistic storm surge scenarios historically encountered. However, due to less developed dune sections and several gaps through which water can flow behind the foredune to the adjacent dike/dune line, the system does not offer a continuous flood protection line. Nevertheless, the foredune provides a certain safety level against wave attack and serves as an additional protective buffer during more severe storm events, potentially relieving the established coastal structures.

4 Discussion

This study investigated the spatio-temporal growth of a geologically young 6.5 km coastal foredune with a decadal perspective and attributed storm surge protection potential based on the FEMA-540 rule by establishing a newly defined CSSL parameter. For clarity, discussion topics are grouped following (1) the new semi-automated dune toe detection procedure; (2) the spatio-temporal investigation of the foredune development and (3) the correlation between identified dune formation and provided coastal storm surge protection.

4.1 Semi-automated dune toe detection

This study presents a new semi-automated DTT method to systematically extract spatial dune toe positions along coastal cross-shore profiles based on specially defined inclination angles, gradients and thresholds. In contrast to conventional methods based on fixed vertical elevations (e.g. applied by Hofstede, 1997; De Vries et al., 2012; Donker et al., 2018; Eichmanns et al., 2021; Masselink et al., 2022; Nicolae Lerma et al., 2022), the approach derives a generic toe determination that considers individual dune profile characteristics and adjacent foreshore elevations. As a result, the proposed method omits the problem of defining a fixed geodetic datum, making comparisons between different coastlines and countries accessible, as the detection relies on physically defined criteria. Moreover, as demonstrated in this study, the application enables a long-term temporal tracking of lateral dune toe shifting as well as vertical dune toe translation over large areas and long periods of dune evolution. This composition of continuous dune toe tracking evolution allows correlation with other external drivers such as SLR, shoreline change and storm surges to dune system responses. In addition, as recently pointed out by Diamantidou et al. (2020), precise dune toe detection can also serve as a useful tool for coastal management when it comes to nourishments or the definition of safety levels against flooding.

The detection method in combination with the defined criteria proved to be spatio-temporally robust with few dune toe outliers (approximately 2% outliers in 2015 using the applied configuration with a cross-shore distance Δx of 150m) over the entire study area. As mentioned by Diamantidou et al. (2020) and demonstrated by applying their second derivative method for the study area, potential outliers can occur due to cross-shore profile anomalies (e.g. sandbars or shallow peaks) along the foreshore leading to major lateral deviations in dune toe tracking seaward from the beach-dune intersection. This was counteracted by defining a minimum dune toe elevation above mean high water, establishing a minimum dune crest elevation of 0.5m above mean high water and starting the dune toe detection from the dune crest in seaward direction. In order to counteract anomalies in the dune profile (multiple dune ridges or shallow peaks at the seaward dune slope), different cross-shore distances Δx were tested and statistically evaluated to apply the best fitting distance for the study area. Therefore, the application of these defined criteria enabled a consistent dune toe tracking for different types of beach-dune profiles (e.g. completely smooth beach profiles, varying beach-dune profiles with multiple shallow peaks).

However, it should be noted that the search algorithm includes no automated filter yet to distinguish between beach-dune systems and other natural (e.g. salt marshes) or artificial elevation (e.g. sea dikes). Therefore, upcoming analyses in other locations also need to be situated in clear beach-dune systems to ensure robust dune toe detection. Depending on local conditions as well as geospatial data coverage and resolution, different configuration adjustments can be applied to enhance specific detection by: (i) changing the minimum peak elevation threshold depending on the seaward beach uniformity; (ii) adaptation of the cross-shore distance Δx related to the size, width and shape of the dune profile and (iii) adjustment of the defined height deviation of 0.1% depending on the seaward dune slope.

4.2 Identified foredune development

The dune analysis procedure outlined in this study has proven to be suitable to systematically analyze vast quantities of geospatial survey data covering extended time periods. The method can be successfully used to track the spatio-temporal development of characteristic geometric dune parameters describing the formation and dynamic growth of a newly arisen foredune system. As demonstrated, the foredune at the Eiderstedt peninsula grew with a mean annual volume increase of 7.4m^3/m over the past decades. A similar long-term dune growth rate along the North Sea has recently been observed at the Belgian coast by Strypsteen et al. (2019) with 6.2m^3/m/yr (range between 0-12.3m^3/m/yr) over a period of 39 years. Furthermore, De Vries et al. (2012) reported on linear dune growth rates at the Holland Coast in the order of 0-40m^3/m/yr over 45 years. Similar to findings by Van IJzendoorn et al. (2021) along the Dutch coast, the analyzed dune toe elevation of 1.1 cm/yr was approximately 4 to 5 times higher compared to local SLR of 0.25 cm/yr, resulting in a *Dune Translation Index* (DTI) of 4.4 and therefore likely outpacing SLR. However, it is noted that mean wind directions and sediment supply at those locations may not easily be compared and further research is warranted into these correlations.

A precise analysis of the landward dune toe was not feasible due to the landward bordering salt marsh and the dike/dune line, resulting in a reduced number of identified and evaluated dune volumes. However, the observed ongoing increase in dune height and volume as well as the progradation of the seaward dune toe indicate that the dune development is not yet complete and that the dune will continue to grow in the near future, depending on sediment supply from the beach and storm surge history.

The geospatial processing of the survey data resulted in very small elevation deviations (see inverse-triangulations in Supplementary Material). The calculated least square error increases for more recent data sets, as the foredune developed over time and a less homogeneous surface elevation has evolved. Least square errors range from 0m to 8.6×10^{-14} m from the initial to the latest data set respectively. Given the small deviation errors for later data sets on a magnitude of ≤1% compared to the absolute dune heights, the authors regard this influence to be negligible on the overall results. Similar to studies by Donker et al. (2018) and Nicolae Lerma et al. (2022), the high spatial resolution with a generated grid cell size of 1.0m enabled a robust dune analysis and the identification of high spatial alongshore variability in foredune growth over the years. According to Corbau et al. (2015), who also observed alongshore dune variations along the Italian coast, the variability is primarily controlled by sediment budget, wind-wave orientation to the beach and potential human impacts. In the course of geodata processing, a 6.4 km long geotransect was defined, following the overall convex shaped curvature of the foredune crest line along its north-south axis, in order to numerically construct normal elevation profiles covering the entire study area. In this regard, it should be noted that the proposed geotransect definition is only suitable for normal and convex shaped coasts, as normal profiles constructed along concave shaped coastlines such as bays could intersect within the area of interest, potentially doubling the analysis of specific data points and skewing results.

Due to the overall low and also unevenly distributed temporal resolution of available geospatial data over the years, a reliable correlation between observed dune growth and potential consequences of encountered storm surge events was not yet possible. As shown by Castelle et al. (2017), who analyzed survey data sampled every 2 to 4 weeks over a time span of approximately 10 years, high temporal resolution involving multiple annual measurements enables a comprehensive investigation of beach-dune erosion and post-storm recovery. In addition, Nicolae Lerma et al. (2022) recently demonstrated that even annual geodata collections can be sufficient to highlight insights into beach-dune recovery after an erosive winter season.

Furthermore, this study does not primarily focus on potential drivers of dune development, which opens some scientific gaps for further research. Besides correlating dune formation and growth with local SLR (e.g. Van IJzendoorn et al., 2021; Masselink et al., 2022), additional influencing factors such as changing wave and wind conditions (e.g. Corbau et al., 2015; He et al., 2022) can be examined in more detail. Building on a finding by Strypsteen et al. (2019) that natural dune growth is primarily caused by aeolian sediment transport from the beach, local wind data can be utilized to correlate aeolian transport rates with dune growth. In parallel to this study, ongoing research concerns the historical evolution of sandbar migration in the extended area around the Eiderstedt peninsula and highlights significant beach growth over the past half century (Soares et al., 2022), possibly increasing the aeolian fetch length and enhancing aeolian sediment transport. In this context, further focus can be directed towards biophysical feedback between sand supply and local vegetation changes influencing the foredune development (similar to Zarnetske et al., 2015).

4.3 Foredune correlated storm surge protection

Building on a comprehensive foredune analysis, this study provides a first analytical method to relate coastal protection potential to spatio-temporal dune development. To enable an adequate assessment, the approach requires considerable simplifications compared to established numerical models by neglecting physical processes (e.g. wave characteristics and storm duration) as well as specific boundary conditions (e.g.

fronting beach profile). Furthermore, the iterative determination of CSSLs along different cross-shore elevation profiles does not consider specific dune forms (e.g. varying seaward dune slope inclinations or presence of shallow dune ridges seaward from the crest), as the definition of the vertical boundary line depends exclusively on the lateral position of the dune crest. According to Wootton et al. (2016), it should also be noted that new post-storm survey observations indicate the need for an increased minimum cross-sectional frontal dune area to (a) withstand significant dune erosion under future conditions and (b) account for cumulative effects of sequential storm events during short time periods (FEMA, 2011). Despite an outlined recommendation to increase the area to 1100 cubic feet per linear foot (approximately 100m^3/m), this study still applies the existing rule with a minimum threshold of 540 cubic feet per linear foot (approximately 50m^3/m). However, within the framework of upcoming studies, this recommendation can simply be inserted into the procedure by adjusting the threshold value.

Although the adapted FEMA-540 rule is not suitable to investigate dune erosion processes and quantify erosion rates, the new defined CSSL parameter facilitates a straightforward approach to systematically estimate storm surge protection levels for coastal dunes in large coastal areas. Besides the previously highlighted correlation to coastal dune evolution, the approach can be a valuable tool in (i) forecasting vulnerable alongshore dune sections (shallow dune ridges, gaps); (ii) identifying dune sections with a need for reinforcement [e.g. additional sand nourishment (Brand et al., 2022), sand fencing (Eichmanns et al., 2021), hybrid dune core strengthening (Nordstrom, 2019)] and (iii) tracking post-storm related vulnerable sections.

As recently reported by Figlus (2022), the dynamic nature of coastal dunes is the most important aspect when discussing dunes in coastal flood-risk reduction schemes. In this context, one significant factor is the non-uniform spatio-temporal dune growth demonstrated in this study, which leads to alongshore variations in dune height and volume. As a consequence, size discontinuities along the foredune have a major influence on the provided storm surge protection potential. Thereby, it is essential to distinguish between protection against wave attack and protection against flooding. Although a substantial part of the developed foredune provides verifiable protection against wave attack during storm surges, the dune does not offer a continuous barrier against flooding. Since several shallow dune ridges and gaps interrupt the foredune line, water can flow through these sections during storm events and reach the adjacent dike/dune line. In this context, further research can be conducted to investigate the development of blowouts and simulate wave-induced water flow through existing dune gaps.

Furthermore, Figlus (2022) pointed out that some countries (e.g. the United States and the Netherlands) already incorporate sand dunes into the design of coastal risk reduction projects. Against the background of climate change, coastal squeeze and an increasing demand for nature based solutions, the introduced CSSL enables the possibility to include foredunes in existing protection policies and guidelines as initial barrier lines against moderate storm surges or additional buffers against more severe storm events. In addition, the CSSL parameter offers an approach to compare storm surge protection of coastal dunes and sea dikes against specific SSLs, a fact that has mostly been neglected by coastal protection authorities in the past.

Data availability statement

The raw data supporting the conclusions of this article will be made available by the authors, without undue reservation.

Author contributions

BM conceived the conceptualization and prepared the original draft of the manuscript with input from OL, BM, and TB developed the methodologies to systematically detect dune toes, analyze specific dune parameters and derive potential storm surge protection. OL supported this procedure by processing the supplied geospatial data into digital elevation models and designing the corresponding figures. BM conducted the analysis procedure with support from TB and visualized the obtained results. OL, TB, VK, and NG contributed to the manuscript revisions and final editing. NG supervised the entire study, obtained and administered the funding. All authors approved the submitted version.

Funding

This research was funded by the German Federal Agency for Nature Conservation (BfN), the German Federal Ministry for the Environment, Nature Conservation, Nuclear Safety and Consumer Protection (BMUV) and the Ministry for Energy Transition, Climate Protection, Environment and Nature (MELUR) in the framework of the joint-research project "Sandküste St. Peter-Ording" (FKZ 3520685C16). We acknowledge support by the Open Access Publication Funds of Technische Universität Braunschweig.

Acknowledgments

The authors would like to acknowledge the project "Sandküste St. Peter-Ording" (FZK 3520685C16) and the valuable knowledge exchange with involved project partners. Further, we thank the LKN.SH for providing digital terrain data

as well as the BfG for providing water level data from several gauging stations. Special thanks goes to David Schürenkamp who was instrumental in the preparation of the funding proposal and initiation of the research project.

Conflict of interest

The authors declare that the research was conducted in the absence of any commercial or financial relationships that could be construed as a potential conflict of interest.

Publisher's note

All claims expressed in this article are solely those of the authors and do not necessarily represent those of their affiliated organizations, or those of the publisher, the editors and the reviewers. Any product that may be evaluated in this article, or claim that may be made by its manufacturer, is not guaranteed or endorsed by the publisher.

Supplementary material

The Supplementary Material for this article can be found online at: https://www.frontiersin.org/articles/10.3389/fmars.2022.1020351/full#supplementary-material

SUPPLEMENTARY TABLE 1
Overview of all analyzed dune parameters.

SUPPLEMENTARY DATA SHEET
Inverse-triangulations for all DEMs.

References

Arens, S. M. (1996). Patterns of sand transport on vegetated foredunes. *Geomorphology* 17, 339–350. doi: 10.1016/0169-555X(96)00016-5

Arens, S. M. (1997). Transport rates and volume changes in a coastal foredune on a Dutch wadden island. *J. Coast. Conserv.* 3, 49–56. doi: 10.1007/BF03341352

Arns, A., Wahl, T., Dangendorf, S., and Jensen, J. (2015). The impact of sea level rise on storm surge water levels in the northern part of the German bight. *Coast. Eng.* 96, 118–131. doi: 10.1016/j.coastaleng.2014.12.002

Barbier, E., Hacker, S., Kennedy, C., Koch, E., Stier, A., and Silliman, B. (2011). The value of estuarine and coastal ecosystem services. *Ecol. Monogr.* 81, 169–193. doi: 10.1890/10-1510.1

Bauer, B. O., Davidson-Arnott, R. G. D., Hesp, P. A., Namikas, S. L., Ollerhead, J., and Walker, I. J. (2009). Aeolian sediment transport on a beach: Surface moisture, wind fetch, and mean transport. *Geomorphology* 105, 106–116. doi: 10.1016/j.geomorph.2008.02.016

Bell, R. J., Gray, S. L., and Jones, O. P. (2017). North Atlantic storm driving of extreme wave heights in the north Sea. *J. Geophysical Research: Oceans* 122, 3253–3268. doi: 10.1002/2016JC012501

Brand, E., Ramaekers, G., and Lodder, Q. (2022). Dutch Experience with sand nourishments for dynamic coastline conservation – an operational overview. *Ocean Coast. Manage.* 217, 106008. doi: 10.1016/j.ocecoaman.2021.106008

Brantley, S., Bissett, S., Young, D., Wolner, C., and Moore, L. (2014). Barrier island morphology and sediment characteristics affect the recovery of dune building grasses following storm-induced overwash. *PloS One* 9, e104747. doi: 10.1371/journal.pone.0104747

Brodie, K., Conery, I., Cohn, N., Spore, N., and Palmsten, M. (2019). Spatial variability of coastal foredune evolution, part a: Timescales of months to years. *J. Mar. Sci. Eng.* 7, 124. doi: 10.3390/jmse7050124

Bruun, P. (1962). Sea-Level rise as a cause of shore erosion. *J. Waterways Harbors Division* 88, 117–130. doi: 10.1061/JWHEAU.0000252

Castelle, B., Bujan, S., Ferreira, S., and Dodet, G. (2017). Foredune morphological changes and beach recovery from the extreme 2013/2014 winter at a high-energy sandy coast. *Mar. Geology* 385, 41–55. doi: 10.1016/j.margeo.2016.12.006

Cohn, N., Ruggiero, P., de Vries, S., and Kaminsky, G. M. (2018). New insights on coastal foredune growth: The relative contributions of marine and aeolian processes. *Geophysical Res. Lett.* 45, 4965–4973. doi: 10.1029/2018GL077836

Corbau, C., Simeoni, U., Melchiorre, M., Rodella, I., and Utizi, K. (2015). Regional variability of coastal dunes observed along the Emilia-romagna littoral, Italy. *Aeolian Res.* 18, 169–183. doi: 10.1016/j.aeolia.2015.07.001

Davidson-Arnott, R., and Law, M. (1996). Measurement and prediction of long-term sediment supply to coastal foredunes. *J. Coast. Res.* 12, 654–663.

Delgado-Fernandez, I., and Davidson-Arnott, R. (2011). Meso-scale aeolian sediment input to coastal dunes: The nature of aeolian transport events. *Geomorphology* 126, 217–232. doi: 10.1016/j.geomorph.2010.11.005

De Vries, S., Southgate, H. N., Kanning, W., and Ranasinghe, R. (2012). Dune behavior and aeolian transport on decadal timescales. *Coast. Eng.* 67, 41–53. doi: 10.1016/j.coastaleng.2012.04.002

Diamantidou, E., Santinelli, G., Giardino, A., Stronkhorst, J., and de Vries, S. (2020). An automatic procedure for dune foot position detection: Application to the Dutch coast. *J. Coast. Res.* 36, 668–675. doi: 10.2112/JCOASTRES-D-19-00056.1

Dingler, J. R., Hsu, S. A., and Reiss, T. E. (1992). Theoretical and measured aeolian sand transport on a barrier island, Louisiana, USA. *Sedimentology* 39, 1031–1043. doi: 10.1111/j.1365-3091.1992.tb01995.x

Dissanayake, P., Brown, J., Sibbertsen, P., and Winter, C. (2021). Using a two-step framework for the investigation of storm impacted beach/dune erosion. *Coast. Eng.* 168, 103939. doi: 10.1016/j.coastaleng.2021.103939

Donker, J., van Maarseveen, M., and Ruessink, G. (2018). Spatio-temporal variations in foredune dynamics determined with mobile laser scanning. *J. Mar. Sci. Eng.* 6, 126. doi: 10.3390/jmse6040126

Durán, O., and Moore, L. J. (2013). Vegetation controls on the maximum size of coastal dunes. *Proc. Natl. Acad. Sci.* 110, 17217–17222. doi: 10.1073/pnas.1307580110

Eichmanns, C., Lechthaler, S., Zander, W., Pérez, M., Blum, H., Thorenz, F., et al. (2021). Sand trapping fences as a nature-based solution for coastal protection: An international review with a focus on installations in Germany. *Environments* 8, 135. doi: 10.3390/environments8120135

Elsayed, S. M., Gijsman, R., Schlurmann, T., and Goseberg, N. (2022). Nonhydrostatic numerical modeling of fixed and mobile barred beaches: Limitations of depth-averaged wave resolving models around sandbars. *J. Waterway Port Coastal Ocean Eng.* 148, 04021045. doi: 10.1061/(ASCE)WW.1943-5460.0000685

EMODnet Bathymetry Consortium (2020). *Emodnet digital bathymetry (dtm 2020)*, Dataset [Oostende, Belgium: European Directorate-General for Maritime Affairs and Fisheries (DG MARE)]. doi: 10.12770/bb6a87dd-e579-4036-abe1-e649cea9881a

Falkenrich, P., Wilson, J., Nistor, I., Goseberg, N., Cornett, A., and Mohammadian, A. (2021). Nature-based coastal protection by Large woody debris as compared to seawalls: A physical model study of beach morphology and wave reflection. *Water* 13, 2020. doi: 10.3390/w13152020

FEMA (2011). *Coastal construction manual principles and practices of planning, siting, designing, constructing, and maintaining residential buildings in coastal areas*

(Fourth edition). 4 (Washington, DC, USA: CreateSpace Independent Publishing Platform). Federal Emergency Managament Agency.

Figlus, J. (2022). "Designing and implementing coastal dunes for flood risk reduction," in *Coastal flood risk reduction* (Elsevier: Coastal Flood Risk Reduction, The Netherlands and the U.S. Upper Texas Coast), 287–301. doi: 10.1016/B978-0-323-85251-7.00021-4

Gao, J., Kennedy, D. M., and Konlechner, T. M. (2020). Coastal dune mobility over the past century: A global review. *Prog. Phys. Geography: Earth Environ.* 44, 814–836. doi: 10.1177/0309133320919612

Gencarelli, R., Tomasicchio, G., Kobayashi, N., and Johnson, B. (2008). Beach profile evolution and dune erosion due to the impact of hurricane Isabel. *Proceedings of 31st International Conference on Coastal Engineering, ASCE, Hamburg, Germany.* 1697–1709. doi: 10.1142/9789814277426_141

Goldstein, E. B., and Moore, L. J. (2016). Stability and bistability in a one-dimensional model of coastal foredune height. *J. Geophysical Research: Earth Surface* 121, 964–977. doi: 10.1002/2015JF003783

Goldstein, E. B., Moore, L. J., and Durán Vinent, O. (2017). Lateral vegetation growth rates exert control on coastal foredune hummockiness and coalescing time. *Earth surface dynamics* 5, 417–427. doi: 10.5194/esurf-5-417-2017

Grabemann, I., Groll, N., Möller, J., and Weisse, R. (2015). Climate change impact on north Sea wave conditions: a consistent analysis of ten projections. *Ocean Dynamics* 65, 255–267. doi: 10.1007/s10236-014-0800-z

Gracia, A., Rangel-Buitrago, N., Oakley, J. A., and Williams, A. T. (2018). Use of ecosystems in coastal erosion management. *Ocean Coast. Manage.* 156, 277–289. doi: 10.1016/j.ocecoaman.2017.07.009

Grilliot, M. J., Walker, I. J., and Bauer, B. O. (2019). The role of Large woody debris in beach-dune interaction. *J. Geophysical Research: Earth Surface* 124, 2854–2876. doi: 10.1029/2019JF005120

Hallin, C., Larson, M., and Hanson, H. (2019). Simulating beach and dune evolution at decadal to centennial scale under rising sea levels. *PloS One* 14, 1–30. doi: 10.1371/journal.pone.0215651

Harley, M. D., Masselink, G., Ruiz de Alegría-Arzaburu, A., Valiente, N. G., and Scott, T. (2022). Single extreme storm sequence can offset decades of shoreline retreat projected to result from sea-level rise. *Commun. Earth Environ.* 3, 1–11. doi: 10.1038/s43247-022-00437-2

He, Y., Cai, F., Liu, J., Qi, H., Li, B., Zhao, S., et al. (2022). Foredune height variations along the western coast of Taiwan strait. *Earth Surf. Process. Landforms.* 47, 2765–2778. doi: 10.1002/esp.5422. Article esp.5422.

Héquette, A., Ruz, M.-H., Zemmour, A., Marin, D., Cartier, A., and Sipka, V. (2019). Alongshore variability in coastal dune erosion and post-storm recovery, northern coast of France. *J. Coast. Res.* 88, 25–45. doi: 10.2112/SI88-004.1

Heslenfeld, P., Jungerius, P. D., and Klijn, J. A. (2008). "European Coastal dunes: Ecological values, threats, opportunities and policy development," in *Coastal dunes. ecological studies*, vol. 171 . Eds. M. Martínez and N. Psuty (Berlin, Heidelberg: Springer), 335–351. doi: 10.1007/978-3-540-74002-5_20

Hesp, P. (1988). Surfzone, beach and fordune interactions on the Australian southeast coast. *J. Coast. Res.* 3, 15–25.

Hesp, P. (2002). Foredunes and blowouts: initiation, geomorphology and dynamics. *Geomorphology* 48, 245–268. doi: 10.1016/S0169-555X(02)00184-8

Hesp, P. (2013). A 34 year record of foredune evolution, dark point, NSW, Australia. *J. Coast. Res.* 65, 1295–1300. doi: 10.2112/SI65-219.1

Hofstede, J. L. A. (1997). Morphologie des st. Peter-Ording-Sandes. *Die Küste* 59, 143–171.

Houser, C., Wernette, P., Rentschlar, E., Jones, H., Hammond, B., and Trimble, S. (2015). Post-storm beach and dune recovery: Implications for barrier island resilience. *Geomorphology* 234, 54–63. doi: 10.1016/j.geomorph.2014.12.044

Itzkin, M., Moore, L. J., Ruggiero, P., Hacker, S. D., and Biel, R. G. (2021). The relative influence of dune aspect ratio and beach width on dune erosion as a function of storm duration and surge level. *Earth Surface Dynamics* 9, 1223–1237. doi: 10.5194/esurf-9-1223-2021

Jackson, N. L., Sherman, D., Hesp, P., Klein, A. H., Ballasteros, F., and Nordstrom, K. (2006). Small-scale spatial variations in aeolian sediment transport on a fine-sand beach. *J. Coast. Res.* 39, 379–383.

Jänicke, L., Ebener, A., Dangendorf, S., Arns, A., Schindelegger, M., Niehüser, S., et al. (2021). Assessment of tidal range changes in the north Sea from 1958 to 2014. *J. Geophysical Research: Oceans* 126, e2020JC016456. doi: 10.1029/2020JC016456

Janssen, M. S., and Miller, J. K. (2022). The dune engineering demand parameter and applications to forecasting dune impacts. *J. Mar. Sci. Eng.* 10, 234. doi: 10.3390/jmse10020234

Jensen, J. (2020). Retrospektive der meeresspiegelforschung in deutschland. *Hydrografische Nachrichten* 115, 18–26. doi: 10.23784/HN115-03

Jensen, J., and Müller-Navarra, J. H. (2008). Storm surges on the german coast. *Die Küste* 74, 92–124.

Keijsers, J. G. S., Giardino, A., Poortinga, A., Mulder, J. P. M., Riksen, M. J. P. M., and Santinelli, G. (2015). Adaptation strategies to maintain dunes as flexible coastal flood defense in the Netherlands. *Mitigation Adaptation Strategies Global Change* 20, 913–928. doi: 10.1007/s11027-014-9579-y

Kobayashi, N., Agarwal, A., and Johnson, B. D. (2007). Longshore current and sediment transport on beaches. *J. Waterway Port Coastal Ocean Eng.* 133, 296–304. doi: 10.1061/(ASCE)0733-950X(2007)133:4(296

Kriebel, D. L., and Dean, R. G. (1993). Convolution method for time-dependent beach-profile response. *J. Waterway Port Coastal Ocean Eng.* 119, 204–226. doi: 10.1061/(ASCE)0733-950X(1993)119:2(204

Larson, M., Erikson, L., and Hanson, H. (2004). An analytical model to predict dune erosion due to wave impact. *Coast. Eng.* 51, 675–696. doi: 10.1016/j.coastaleng.2004.07.003

Levin, N., Jablon, P.-E., Phinn, S., and Collins, K. (2017). Coastal dune activity and foredune formation on moreton island, Australia 1944–2015. *Aeolian Res.* 25, 107–121. doi: 10.1016/j.aeolia.2017.03.005

Mariotti, G., and Hein, C. J. (2022). Lag in response of coastal barrier-island retreat to sea-level rise. *Nat. Geosci* 15, 633–638. doi: 10.1038/s41561-022-00980-9

Masselink, G., Brooks, S., Poate, T., Stokes, C., and Scott, T. (2022). Coastal dune dynamics in embayed settings with sea-level rise – examples from the exposed and macrotidal north coast of SW England. *Mar. Geology* 450, 106853. doi: 10.1016/j.margeo.2022.106853

Maximiliano-Cordova, C., Martínez, M. L., Silva, R., Hesp, P. A., Guevara, R., and Landgrave, R. (2021). Assessing the impact of a winter storm on the beach and dune systems and erosion mitigation by plants. *Front. Mar. Sci.* 8. doi: 10.3389/fmars.2021.734036

McLean, R., and Shen, J.-S. (2006). From foreshore to foredune: Foredune development over the last 30 years at moruya beach, new south Wales, Australia. *J. Coast. Res.* 22, 28–36. doi: 10.2112/05A-0003.1

MELUR (2013). "Generalplan küstenschutz des landes schleswig-Holstein," in *Fortschreibung 2012* (Kiel, Germany: Ministerium für Energiewende, Landwirtschaft, Umwelt und ländliche Räume des Landes Schleswig-Holstein). MELUR.

Miocic, J. M., Sah, R., Chawchai, S., Surakiatchai, P., Choowong, M., and Preusser, F. (2022). High resolution luminescence chronology of coastal dune deposits near chumphon, Western gulf of Thailand. *Aeolian Res.* 56, 100797. doi: 10.1016/j.aeolia.2022.100797

Miot da Silva, G., and Hesp, P. (2010). Coastline orientation, aeolian sediment transport and foredune and dunefield dynamics of moçambique beach, southern Brazil. *Geomorphology* 120, 258–278. doi: 10.1016/j.geomorph.2010.03.039

Miot da Silva, G., Hesp, P., Peixoto, J., and Dillenburg, S. R. (2008). Foredune vegetation patterns and alongshore environmental gradients: Moçambique beach, Santa catarina island, Brazil. *Earth Surf. Process. Landforms* 33, 1557–1573. doi: 10.1002/esp.1633

MLR (2001). *Generalplan küstenschutz integriertes küstenschutzmanagement in schleswig-Holstein* (Kiel, Germany: Ministerium für ländliche Räume, Landesplanung, Landwirtschaft und Tourismus des Landes Schleswig-Holstein). MLR.

Montreuil, A.-L., Bullard, J. E., Chandler, J. H., and Millett, J. (2013). Decadal and seasonal development of embryo dunes on an accreting macrotidal beach: North Lincolnshire, UK. *Earth Surf. Process. Landforms* 38, 1851–1868. doi: 10.1002/esp.3432

Mull, J., and Ruggiero, P. (2014). Estimating storm-induced dune erosion and overtopping along U.S. West coast beaches. *J. Coast. Res.* 298, 1173–1187. doi: 10.2112/JCOASTRES-D-13-00178.1

Nehren, U., Thai, H. H. D., Marfai, M. A., Raedig, C., Alfonso, S., Sartohadi, J., et al. (2016). "Ecosystem services of coastal dune systems for hazard mitigation: Case studies from vietnam, indonesia, and chile," in *Ecosystem-based disaster risk reduction and adaptation in practice*. Eds. F. G. Renaud, K. Sudmeier-Rieux, M. Estrella and U. Nehren (Cham: Springer International Publishing), 401–433. doi: 10.1007/978-3-319-43633-3_18

Nicolae Lerma, A., Castelle, B., Marieu, V., Robinet, A., Bulteau, T., Bernon, N., et al. (2022). Decadal beach-dune profile monitoring along a 230-km high-energy sandy coast: Aquitaine, southwest France. *Appl. Geogr.* 139, 102645. doi: 10.1016/j.apgeog.2022.102645

Nordstrom, K. F. (2019). Coastal dunes with resistant cores. *J. Coast. Conserv.* 23, 227–237. doi: 10.1007/s11852-018-0653-6

Nordstrom, K. F., Bauer, B. O., Davidson-Arnott, R. G. D., Gares, P. A., Carter, R. W. G., Jackson, D. W. T., et al. (1996). Offshore aeolian transport across a beach: Carrick Finn strand, Ireland. *J. Coast. Res.* 12, 664–672.

Ollerhead, J., Davidson-Arnott, R., Walker, I. J., and Mathew, S. (2013). Annual to decadal morphodynamics of the foredune system at Greenwich dunes, prince Edward island, Canada. *Earth Surface Processes Landforms* 38, 284–298. doi: 10.1002/esp.3327

Pellón, E., Almeida, L. R., González, M., and Medina, R. (2020). Relationship between foredune profile morphology and aeolian and marine dynamics: A

conceptual model. *Geomorphology* 351, 106984. doi: 10.1016/j.geomorph.2019.106984

Pye, K., and Blott, S. (2008). Decadal-scale variation in dune erosion and accretion rates: An investigation of the significance of changing storm tide frequency and magnitude on the sefton coast, UK. *Geomorphology* 102, 652–666. doi: 10.1016/j.geomorph.2008.06.011

Rader, A. M., Pickart, A. J., Walker, I. J., Hesp, P. A., and Bauer, B. O. (2018). Foredune morphodynamics and sediment budgets at seasonal to decadal scales: Humboldt bay national wildlife refuge, California, USA. *Geomorphology* 318, 69–87. doi: 10.1016/j.geomorph.2018.06.003

Roelvink, D., Reniers, A., van Dongeren, A., van Thiel de Vries, J., McCall, R., and Lescinski, J. (2009). Modelling storm impacts on beaches, dunes and barrier islands. *Coast. Eng.* 56, 1133–1152. doi: 10.1016/j.coastaleng.2009.08.006

Sallenger, A. H. (2000). Storm impact scale for barrier islands. *J. Coast. Res.* 16, 890–895.

Santos, V. M., Wahl, T., Long, J. W., Passeri, D. L., and Plant, N. G. (2019). Combining numerical and statistical models to predict storm-induced dune erosion. *J. Geophysical Research: Earth Surface* 124, 1817–1834. doi: 10.1029/2019JF005016

Seeliger, U., Cordazzo, C. V., Oliveira, C. P. L., and Seeliger, M. (2000). Long-term changes of coastal foredunes in the southwest Atlantic. *J. Coast. Res.* 16, 1068–1072.

Sievers, J., Malte, R., and Milbradt, P. (2020). *Easygsh-db: Bathymetrie, (1996-2016)*, Dataset (Hamburg, Germany: BAW, Federal Waterways Engineering and Research Institute). doi: 10.48437/02.2020.K2.7000.0002

Sloss, C. R., Patrick, H., and Michael, S. (2012). Coastal dunes: Aeolian transport. *Nat. Educ. Knowledge* 3.

Soares, C., Herrling, G., and Winter, C. (2022). *Tracing 100 years of morphological development of the sankt Peter-ording sand, a barrier beach system in the north Frisian wadden Sea* (Vienna, Austria: EGU - European Geosciences Union e.V., Gillian D'Souza, Kastenbauerstr. Munich, Germany), 23–27. May 2022, EGU22-9380: EGU General Assembly 2022. doi: 10.5194/egusphere-egu22-9380

Splinter, K. D., Kearney, E. T., and Turner, I. L. (2018). Drivers of alongshore variable dune erosion during a storm event: Observations and modelling. *Coast. Eng.* 131, 31–41. doi: 10.1016/j.coastaleng.2017.10.011

Strypsteen, G., Houthuys, R., and Rauwoens, P. (2019). Dune volume changes at decadal timescales and its relation with potential aeolian transport. *J. Mar. Sci. Eng.* 7, 357. doi: 10.3390/jmse7100357

Temmerman, S., Meire, P., Bouma, T., Herman, P., Ysebaert, T., and de Vriend, H. (2013). Ecosystem-based coastal defence in the face of global change. *Nature* 504, 79–83. doi: 10.1038/nature12859

Tylkowski, J. (2017). The temporal and spatial variability of coastal dune erosion in the polish Baltic coastal zone. *Baltica* 30, 97–106. doi: 10.5200/baltica.2017.30.11

Van IJzendoorn, C. O., de Vries, S., Hallin, C., and Hesp, P. A. (2021). Sea Level rise outpaced by vertical dune toe translation on prograding coasts. *Sci. Rep.* 11, 12792. doi: 10.1038/s41598-021-92150-x

Van Puijenbroek, M. E., Limpens, J., de Groot, A. V., Riksen, M. J., Gleichman, M., Slim, P. A., et al. (2017). Embryo dune development drivers: beach morphology, growing season precipitation, and storms. *Earth Surface Processes Landforms* 42, 1733–1744. doi: 10.1002/esp.4144

Van Rijn, L. C. (2009). Prediction of dune erosion due to storms. *Coast. Eng.* 56, 441–457. doi: 10.1016/j.coastaleng.2008.10.006

Vousdoukas, M. I., Mentaschi, L., Voukouvalas, E., Verlaan, M., and Feyen, L. (2017). Extreme sea levels on the rise along europe's coasts. *Earth's Future* 5, 304–323. doi: 10.1002/2016EF000505

Wernette, P., Houser, C., and Bishop, M. P. (2016). An automated approach for extracting barrier island morphology from digital elevation models. *Geomorphology* 262, 1–7. doi: 10.1016/j.geomorph.2016.02.024

Wong, P. P., Losada, I. J., Gattuso, J.-P., Hinkel, J., Khattabi, A., McInnes, K. L., et al. (2014). "Coastal systems and low-lying areas," in *Climate change 2014 impacts, adaptation, and vulnerability. part a: Global and sectoral aspects. contribution of working group II to the fifth assessment report of the intergovernmental panel on climate change*. Eds. C. B. Field, V. R. Barros, D. J. Dokken, K. J. Mach, M. D. Mastrandrea, T. E. Bilir and M. Chatterjee (Cambridge, United Kingdom and New York, NY, USA: Cambridge University Press), 361–409.

Wootton, L., Miller, J., Miller, C., Peek, M., Williams, A., and Rowe, P. (2016). *New Jersey Sea grant consortium dune manual, retrieved from njseagrant.org/dunemanual. 1* (New Jersey, USA: New Jersey Sea Grant Consortium). NJSGC.

Zarnetske, P. L., Ruggiero, P., Seabloom, E. W., and Hacker, S. D. (2015). Coastal foredune evolution: the relative influence of vegetation and sand supply in the US pacific Northwest. *J. R. Society Interface* 12, 20150017. doi: 10.1098/rsif.2015.0017